Steady-Shear Rheology Properties of Polydimethylsiloxane (PDMS) Colloids as a New Contrast Agent for Nuclear Magnetic Resonance Imaging

FU-HU SU,[1] SHIN-SHING SHYU,[1] YI-CHEN CHEN,[1] YWU-JANG FU[2]

[1] Department of Chemical Engineering, National Central University, Chung-Li Taiwan 32054

[2] Department of Textile Science, Van Nung Institute of Technology, Chung-Li Taiwan 32054

Received 4 November 1999; revised 25 July 2000

ABSTRACT: This work investigated the toxicity, the nuclear magnetic resonance (NMR) spectra, the NMR imaging, and the steady-rheology properties concerning polydimethylsiloxane (PDMS) colloids. These experiments illustrate low toxicity, strong NMR signal intensity, as well as clear images, and render the colloids the potential application as contrast agent for gastrointestinal NMR imaging. The steady-shear rheology data are fitted very well by the model $\tau = \tau_0 + A\dot{\gamma}^m$. According to the theory of Princen and Kiss,[12] we found the yield stresses (τ_0) of the colloids are proportional to $\varphi^{1/3}/D$ in $0.72 \leqq \varphi \leqq 0.81$. Based on the model and the definition of the capillary number Ca $= \tau/(\sigma/R)$, a linear relationship between $\log(D)$ and m was discovered if the assumptions that $2\text{Ca}\ \sigma/A$ and $\dot{\gamma}_{\text{eff}}$ are constants are satisfied. We also proved these assumptions are rational in the investigated range $0.62 \leqq \varphi \leqq 0.81$. © 2002 Wiley Periodicals, Inc. J Appl Polym Sci 85: 1888–1896, 2002

Key words: contrast agent; colloid; emulsion; polydimethylsiloxane (PDMS); rheology

INTRODUCTION

Nuclear magnetic resonance (NMR) imaging has been proposed as a clinical diagnostic modality.[1] To enhance the image contrast, a contrast agent is used in this imaging technique. The ongoing developments of contrast agents for NMR imaging have prompted the need for a new class of pharmaceuticals.[2–6] Most of these contrast agents are derived from metal complexes composed of a metal chelate and a metal ion (e.g., iron, manganese, and gadolinium) that can decrease the relaxation times of nearby nuclei via dipolar interactions. However, polymers are seldom applied to this new class of pharmaceuticals. More recently, polydimethylsiloxane (PDMS) has been proposed as a new contrast agent for gastrointestinal NMR imaging.[7] In this article, three molecular structures, including the linear, the branched, and the cyclic, are reported to be available. In addition, the following three advantages are mentioned: (1) diarrhea and flatulence, which are possible side effects of these metal-based compounds, can be reduced; (2) PDMS is an inert, proton-rich polymer because it has two methyl groups in its repeating unit and already has been used as components of dyspepsia remedies; and (3) in the ^{1}H-NMR spectrum, there is an $\sim$ 4.7 ppm chemical shift from PDMS to water, which is usable for "the chemical shift artifact."

Correspondence to: Shin-Shing Shyu (sufuhu@ms56.url.com.tw).

Journal of Applied Polymer Science, Vol. 85, 1888–1896 (2002)

Most conveniently,[7] PDMS is used in the form of an emulsion. It is important to investigate the rheology properties of this new contrast agent to determine the comfort of oral administration and its flowing behavior in the gastrointestinal tract for drug design purposes. Possibly, the intestine could absorb low molecular PDMSs, which would cause toxicity concern. In this article we propose a crosslinked PDMS colloidal solution to overcome this problem. For linear PDMS emulsions, PDMS is dispersed in water in the form of liquid droplets. Contrarily, crosslinked PDMS is in the form of rubber-like solid particles in colloidal solutions. Both emulsions and colloidal solutions come within the scope of colloids.[8] Few works discussed the different rheology properties between both of them.

The rheology properties of colloids are affected by the volume fraction of dispersion phase (φ),[9–13] the radius (R) of the dispersion,[14–16] the packing effects,[17–19] the kinds of surfactants,[20] etc. These properties exhibit peculiar difference when the volume fraction of the dispersed phase, φ, exceeds that of the close-packed-sphere configuration, φ_c. When $\varphi > \varphi_c$, there is a yield stress, τ_0, at a small strain. But the yield stress can not be found if $\varphi < \varphi_c$; therefore, $\varphi_c \approx 0.635$ and $\varphi_c \approx 0.71$ are for monodisperse emulsions[10] and for polydisperse emulsions,[13] respectively. Because $\varphi > \varphi_c$, the viscosity has significant increases with the increase of φ: too high φ to benefit oral administration (due to higher viscosity), and too low φ to obtain desired intensity of NMR signal. Thus, the investigated samples in this work have their φ in the range $0.62 \leqq \varphi \leqq 0.81$, which are around φ_c. In addition, our preliminary experiments indicate that the PDMS colloids have a strong NMR signal, low toxicity and contrast effect for the NMR image of pig's intestine.

EXPERIMENTAL

Materials

Vinyl-terminated PDMS (Gelest, Germany) was used with different molecular weights (M_w) of 17,200, 28,000, 49,500, and 62,700 g/mol for DMS-V25, DMS-V31, DMS-V35, and DMS-V41, respectively. The linear PDMS can react with a crosslinker to form a crosslinked polymer. The crosslinker (HMS151), also from Gelest, Germany, was a methyl hydrosiloxane–dimethylsiloxane block copolymer with multi-hydrosiloxane bonds that are able to react with vinyl group of the PDMS in the presence of a catalyst. The catalyst (PC075), from Huls America (Bristol, PA), is a mixture of platinum-divinyl tetramethyl disiloxane complex and vinyl-terminated PDMS. Tween-80, from Fisher Scientific (Pittsburgh, PA), is a nonionic surfactant with ethyloxide segments, ethyl segments, and hydroxyl groups at chain ends.

Samples

Generally, the crosslink reactions used to crosslink siloxanes can be categorized in four classes: peroxide-induced free radical reactions, condensation reactions, hydrosilylation addition reactions, and hydridosilane–silanol reactions.[21] The hydrosilylation reaction is an addition reaction between a silicon hydrogen (SiH) bond and an unsaturated carbon—carbon bond, catalyzed by a noble metal, typically Pt. The crosslinked PDMS colloid solutions were prepared by the following hydrosilylation:

$$\underset{\text{(PDMS)}}{\equiv\!\text{SiCH}\!=\!\text{CH}_2} + \underset{\text{(HMS151)}}{\text{HSi}\!\equiv} \xrightarrow{\text{Pt(PC075)}} \underset{\text{(crosslinked PDMS)}}{\equiv\!\text{SiCH}_2\text{CH}_2\text{Si}\!\equiv} \quad (1)$$

For preparing crosslinked PDMS colloid solutions, hydrosilylation is more convenient because it can occur at room temperature; comparatively a higher temperature is need for peroxide-induced free radical reactions. Moreover, this reaction has no by-products, whereas condensation reactions and hydridosilane–silanol reactions can generate low molecular products that could possibly contaminate the colloid solutions.

At first, the linear PDMS (or a mixture of the linear PDMS, the crosslinker, and the catalyst) were dispersed in water to form emulsions with a homogenizer (model T25, IKA, Germany). We mixed the solutions at 8000 rpm and 0°C for 10 min. A lower temperature (0°C) was employed to remove the heat and to moderate the chemical reaction. Then, the samples were kept at room temperature for $>$ 1 day to ensure that the hydrosilylation is completed. Finally, the samples have a dispersion phase with the linear PDMS (or the crosslinked PDMS) and a continuous phase with a mixture of water/Tween (80 = 4/1) by weight. The mass ratios of dispersion phase to continuous phase are 80/20, 75/25, 70/30, 65/35,

and 60/40 for to 0.81, 0.77, 0.72, 0.67, and 0.62 volume fraction, respectively. The relation between the mass ratio and the volume fraction is based on $\varphi = V_d/(V_d + V_c) = (M_d/D_d)/(M_d/D_d + M_c/D_c)$, where V_d and V_c are the volumes of dispersion phase and continuous phase, respectively, M_d and M_c are the mass ratios of dispersion phase and continuous phase, respectively, and D_d (0.93) and D_c (1.023) are the specific gravity of dispersion phase and continuous phase, respectively. The samples with the liner PDMS are denoted as yyLN-xx, in which yy is the number of the trade name of PDMS and xx is the volume fraction of dispersion phase. For example, 31LN-81 represents the DMS-V31 (M_w = 28,000) is used and φ = 0.81. Similarly, the crosslinked PDMS colloid solutions are denoted as yyCL-xx. In the disperse phase of the colloid solutions, the contents of HMS151 and Pt are 2.5% by weight and 20 ppm respectively, except the sample (31CL-72), with 49 ppm of Pt for the 3-(4,5-dimethylthiazol-2-yl)-2,5-diphenyltetrazolium bromide (MTT) assay and the nuclear magnetic resonance imaging (NMRI) test.

Measurements

The ^{1}H-NMR spectra were measured with Bruker DRX-200 system at T = 27°C. The proton images were obtained with Bruker Biospec 47/40 system and are the water-selective images of the pig's small intestines immersed in 31CL-72. For T_1-weight image, the total sequence time, TR, was 510 ms and the time to echo, TE, was 20 ms. Meanwhile, TR = 4110 ms and TE = 100 ms were for T_2-weight image. These are tentative *in vitro* experiments to demonstrate that the colloids have the potential to be a new contrast agent for gastrointestinal NMR imaging.

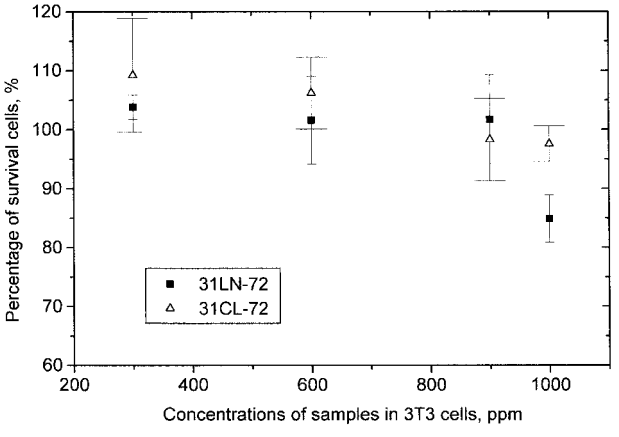

Figure 1 The toxicity of 31EM-72 and 31CL-72 measured with MTT assay and 3T3 cells.

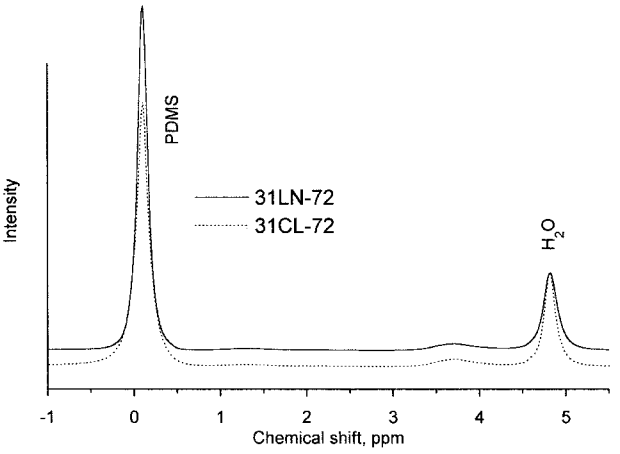

Figure 2 ^{1}H-NMR spectra of 31EM-72 and 31CL-72.

The toxicity of the 31LN-72 and 31CL-72 samples was detected by the MTT reduction assay, which is a tool for quantifying cell death.[22,23] In this experiment, 3T3 cells were used, and different concentrations (from 300 to 1000 ppm) of the samples were added in the cells. The absorption intensities of the cells were recorded (with a microplate reader and at 570 nm) 24 h after the samples had been added to the cells. The percentages of survival cells were determined by dividing the absorption intensity of the cells (with different concentrations of the samples) by that of the control cells (without any additional samples), and five repeat tests were averaged. The deviation of every test from the averaged value is $< 10\%$.

A lighter scattering instrument (Galai Company) was employed to measure the diameters of the droplets (linear PDMS) and the particles (crosslinked PDMS), which are the dispersion phases of these samples. To average the diameter of polydisperse colloids, three conventional definitions[8] are $D_N = \Sigma F_i D_i$, $D_S = (\Sigma F_i D_i^2)^{1/2}$, and $D_V = (\Sigma F_i D_i^3)^{1/3}$, in which F_i is fraction of diameter D_i. Except monodisperse colloids, the relative magnitude of these average diameters are given by the sequence $D_N < D_S < D_V$. In this work, we used D_V to characterize the average diameters of our samples. The reported diameter in this work, D, was an average obtained by repeating tests five times [$D = (1/n)\Sigma D_{Vi}$, $n = 5$, $i = 1 \sim 5$], and the deviations are $< 6\%$ [$(|D_{Vi} - D|)/D < 6\%$].

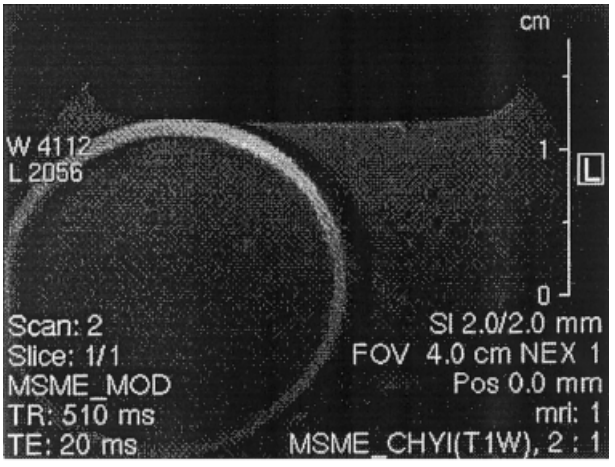

(a)

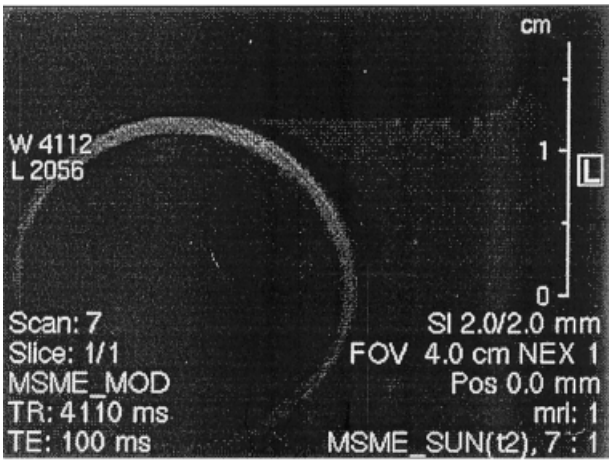

(b)

Figure 3 ^{1}H-NMR images of the pig's intestines immersed in 31CL-72: (a) T_1-weight; (b) T_2-weight.

The steady-shear rheology properties were measured with a RheoStress RS100 (HAAHE Company; Germany). A double cone and plate geometry was employed as the sensor system of these measurements. The different strain rates were swept from 1 to 500 s^{-1}, and the temperature was kept at 25°C.

RESULTS AND DISCUSSION

The results of the MTT assay are shown in Figure 1 and enable a comparison between the toxicity of 31EM-72 and 31CL-72. These results indicate that at $<$ 1000 ppm, both 31EM-72 and 31CL-72 are not harmful to 3T3 cells and the presence of metal Pt does not increase the toxicity. Because PDMS has been used as components of dyspepsia remedies[7] and because the toxicities of 31EM-72 and 31CL-72 are low, the PDMS emulsion and colloidal solution could be a sight for sore eyes in the search for new contrast agents for NMR imaging.

In Figure 2 there are two main peaks in the proton NMR spectra of 31EM-72 and 31CL-72. Their chemical shifts are at 0.11 and 4.82 ppm, which are the characteristic peaks of PDMS and H_2O, respectively. The strong intensity of the PDMS peak shows it is a proton-rich material for proton imaging. The chemical shift difference (~4.7 ppm) between both of them is usable for "the chemical shift artifact," water-selective imaging, and PDMS-selective imaging.

The results of water-selective imaging are shown for the T_1-weight and T_2-weight images in Figures 3a and 3b, respectively. In these figures, the bright circles are the cells of pig's small intestines that are immersed in 31CL-72. The inner surfaces of the both circles are definitely distinguishable. These results reveal that the PDMS colloids have potential application as a contrast agent not only for T_1-weight but also for T_2-weight imaging. In addition to toxicity and NMR properties, the rheology properties of the PDMS colloids are important to consider for their comfort of oral administration and their flowing behavior in the gastrointestinal tract. Therefore, we shall discuss the issue in detail in the following paragraphs.

The effect of molecular weight on the sizes of emulsion droplets is shown in Figure 4. At φ

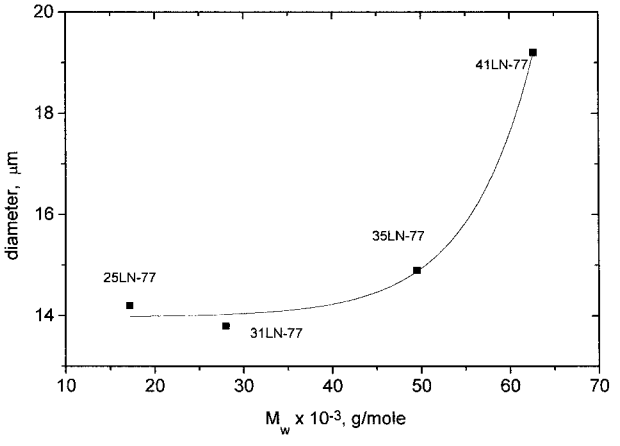

Figure 4 Effects of molecular weight on the diameters of the droplets.

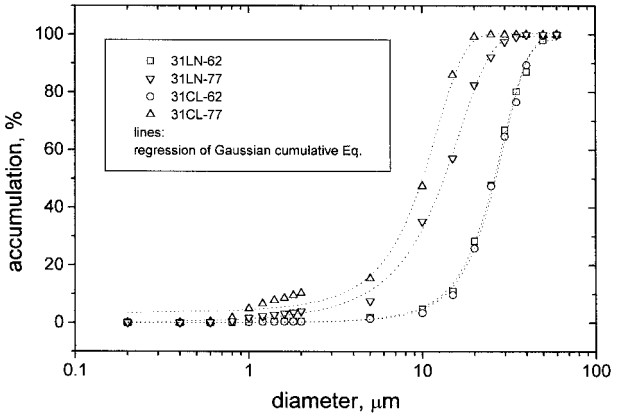

Figure 5 The diameter distributions of 31EM-62, 31EM-77, 31CL-62, and 31CL-77.

= 0.77, we find that the diameter of the droplets increase dramatically as $M_w > 50{,}000$ g/mol. Similar results were found in one experiment of a monodisperse emulsion at $\varphi = 0.7$, which was investigated by Mason et al.[9] During the process of homogenization, the higher viscosity of higher molecular weight PDMS can cause higher stress and more heat, resulting in the chemical reaction of hydrosilylation, which can become violent. We were not able to prepare the crosslinked PDMS colloidal solution with DMS-V35 and DMS-V41. So, we focus on the steady-shear rheology properties of the samples prepared with DMS-V25 and DMS-V31.

Some typical sample diameter distributions are shown in Figure 5. This figure indicates not only that the emulsions but also the colloidal solutions are polydisperse and are in agreement with Gaussian distribution. Additionally, at $\varphi = 0.62$, as shown in Figure 5, the emulsion and the colloidal solution have nearly the same distribution and the same average diameter. These results are attributable to the same volume fraction of the dispersion phase, the same type and concentration of surfactant, and almost no chemical reaction in the process of homogenizing 31CL-72. But the chemical reaction occurred slightly, indicating that 31CL-77 has smaller diameter than 31-EM-77.

The effects of volume fraction on the diameters of the droplets (or the particles) emanated from DMS-V31 are shown in Figure 6, in which the inset is the plot of the data of the samples prepared with DMS-V25. These two data sets indicate that at $\varphi = 0.62$ and with same PDMS, the

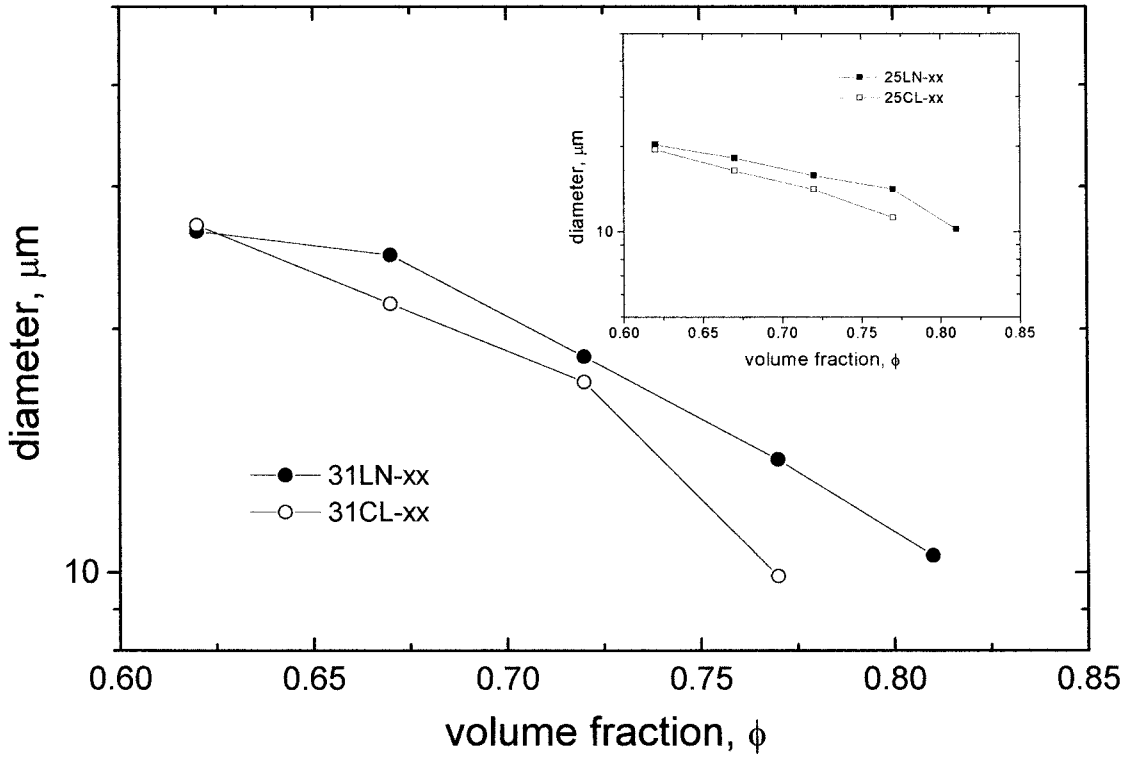

Figure 6 Effects of φ on the diameters of the droplets or the particles.

diameters of the emulsion and the colloidal solution are nearly the same. When $\varphi > 0.62$, the diameters of the colloidal solutions are always smaller than those of the emulsions. In particular, at $\varphi = 0.77$, the difference is larger, indicating that the chemical reaction becomes violent at $\varphi > 0.77$. Therefore, we couldn't prepare yyCL-81 samples because of the violent reaction during homogenization.

The data of shear stress versus strain rate (steady-shear rheology properties) of 31CL-xx are plotted in Figure 7. In this figure, the lines are obtained from fitting these data with

$$\tau = \tau_0 + A\dot{\mathrm{Y}}^{\mathrm{m}} \qquad (2)$$

in which τ is shear stress, τ_0 is yield stress, $\dot{\mathrm{Y}}$ is strain rate, and A and m are constants. In addition, eq. 2 can also be fitted very well to the data of 31EM-xx, 25CL-xx, and 25EM-xx (not shown here). For 31CL-xx and 25CL-xx, $\tau_0 \neq 0$ if $\varphi \geqq 0.72$. For 31EM-xx and 25EM-xx, $\tau_0 \neq 0$ if $\varphi \geqq 0.77$. The yield stresses, τ_0, are yielded by the deformation of the droplets or the particles against their neighbors (because of crowding) and by the attraction of them drawing their neighbors together (because of van der Waal force and hydrogen bonding). The attraction and the deformation lead the samples to behavior of a purely elastic solid at $\tau < \tau_0$. When $\tau > \tau_0$, flow is initiated, and the samples adopt the behavior of shear thinning fluid. By studying the highly concentrated emulsions ($0.83 < \varphi < 0.98$),[12] Princen and Kiss found the relation

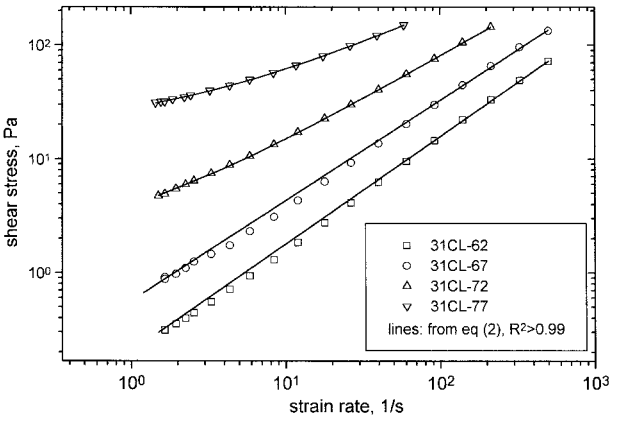

Figure 7 The data of steady-shear experiments of 31CL-xx.

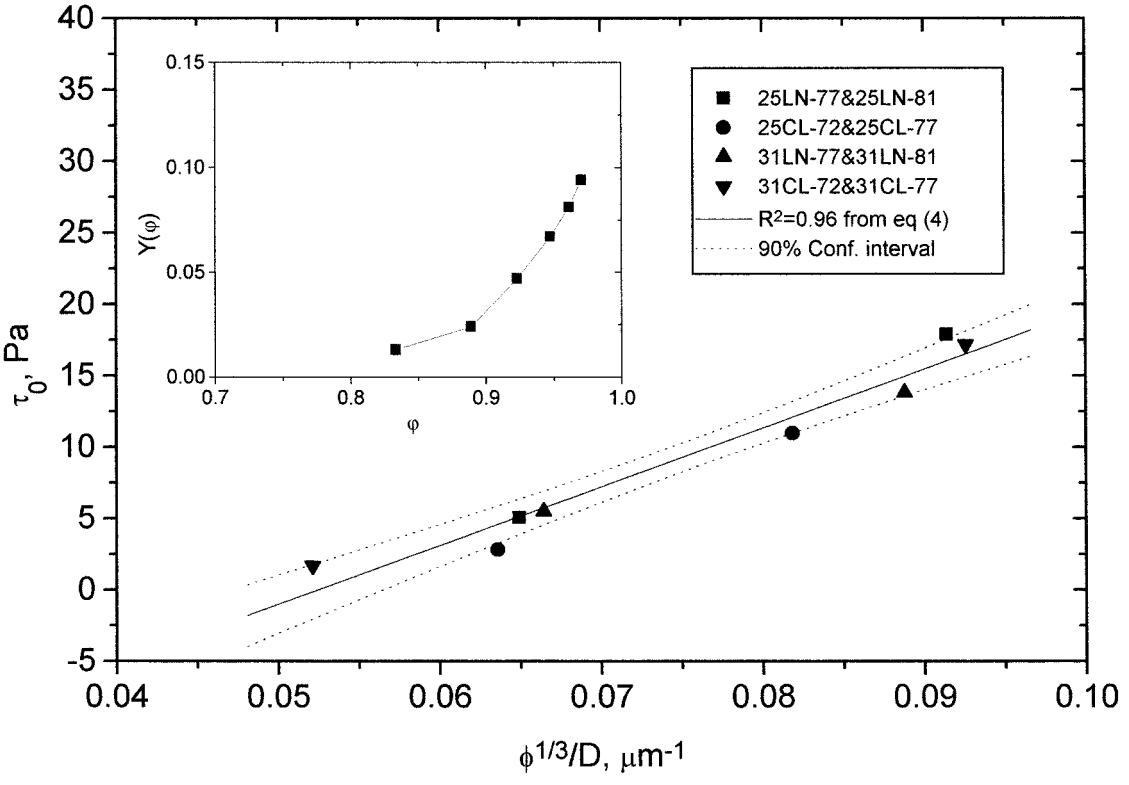

Figure 8 The dependence of the yield stresses on the variations of φ and D. The inset is a plot with the reported data.[12]

$$\tau_0 = \sigma\varphi^{1/3}Y(\varphi)/R \tag{3}$$

where σ is the interfacial tension, R is mean droplet radius, and $Y(\varphi)$ is a function of volume fraction. In this relationship, $Y(\varphi)$ is experimental data, as shown in the inset of Figure 8, indicating that $Y(\varphi)$ increases sharply as $\varphi > 0.9$ and, contrarily, $Y(\varphi)$ decreases as $\varphi < 0.9$. The slight decrease also implies $Y(\varphi)$ has a tendency toward a constant if $\varphi < 0.83$. Thus, $Y(\varphi)$ could be a constant in $0.72 \leqq \varphi \leqq 0.81$, which is the φ range of our samples with $\tau_0 \neq 0$. Because the continuous phases of our samples have the same kind and the same concentration of surfactant, σ could be assumed to be a constant. Consequently, in the range $0.72 \leqq \varphi \leqq 0.81$, eq. 3 can be represented by

$$\tau_0 = C\varphi^{1/3}/D \tag{4}$$

where D ($D = 2R$) is the diameter and C is a constant. The yield stresses of the samples are plotted in Figure 8, showing that they are in agreement with fitting them to eq. 4 and most of them come within the 90% confidence interval of the estimation. This result supports the theory of Princen and Kiss[12] by using the lower volume fraction, which they didn't investigate. As φ approaches unity, the droplets acquire an increasingly pronounced polyhedral shape because of the severe crowding and deformation. Under this circumstance, the deformation dominates the effect on τ_0, and $Y(\varphi)$ increases sharply with increasing φ. Contrarily, when the droplets do not have severe deformation (at lower φ), the attraction dominates the effect on τ_0, and $Y(\varphi)$ has an insignificant dependence on φ. This result explains why in the static state ($\tau < \tau_0$) the rigidity of the particles (the dispersion phase of the colloidal solutions) does not play an important role in affecting τ_0 and the colloidal solutions with $\tau_0 \neq 0$ are in agreement with eq. 4. However, at flowing state ($\tau > \tau_0$), the shear stress τ is significantly influenced by the rigidity, which will be found in the variations of constants A.

Constants A and m of 31EM-xx and 31CL-xx are plotted in Figure 9a and those of 25EM-xx and 25CL-xx are plotted in Figure 9b. The Newtonian fluid has $m = 1$ and $\tau_0 = 0$. But the highly concentrated emulsions ($0.83 < \varphi < 0.98$)[12] have $m = 0.5$ and $\tau_0 \neq 0$. As shown in Figures 9a and 9b, the constant m has a trend toward $m = 0.5$ when φ is increased and toward $m = 1$ when φ is decreased. These phenomena suggest that the

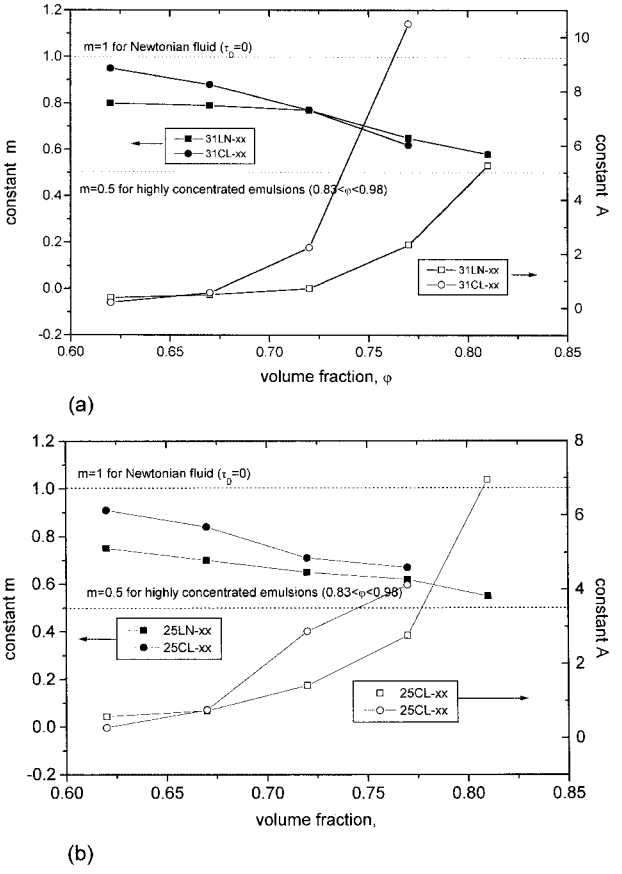

Figure 9 Effects of φ on the constants A and m for (a) 31EM-xx and 31CL-xx; (b) 25EM-xx and 25CL-xx.

rheology properties of our samples come within a transition zone from the Newtonian fluid to the highly concentrated emulsions. Meanwhile, at higher φ, the constant A of the colloidal solutions is obviously higher than that of the emulsions, implying that the rigidity of the disperse phase of the colloidal solutions considerably affects the constant A as well as shear stress τ if $\tau > \tau_0$ and $\varphi > \varphi_c$. Most often, the constants A and m are regarded as empirical constants without physical meanings. We shall relate them to some physical properties, such as volume fraction, average diameter, or shear stress, and we hope that these relations may ultimately provide a basis for the rheology theory of the colloids.

For droplet deformation to occur, the shear stress must overcome the characteristic Laplace pressure (σ/R). The ratio of the shear stress to the Laplace pressure is defined as[9]

$$\mathrm{Ca} = \tau/(\sigma/R) \tag{5}$$

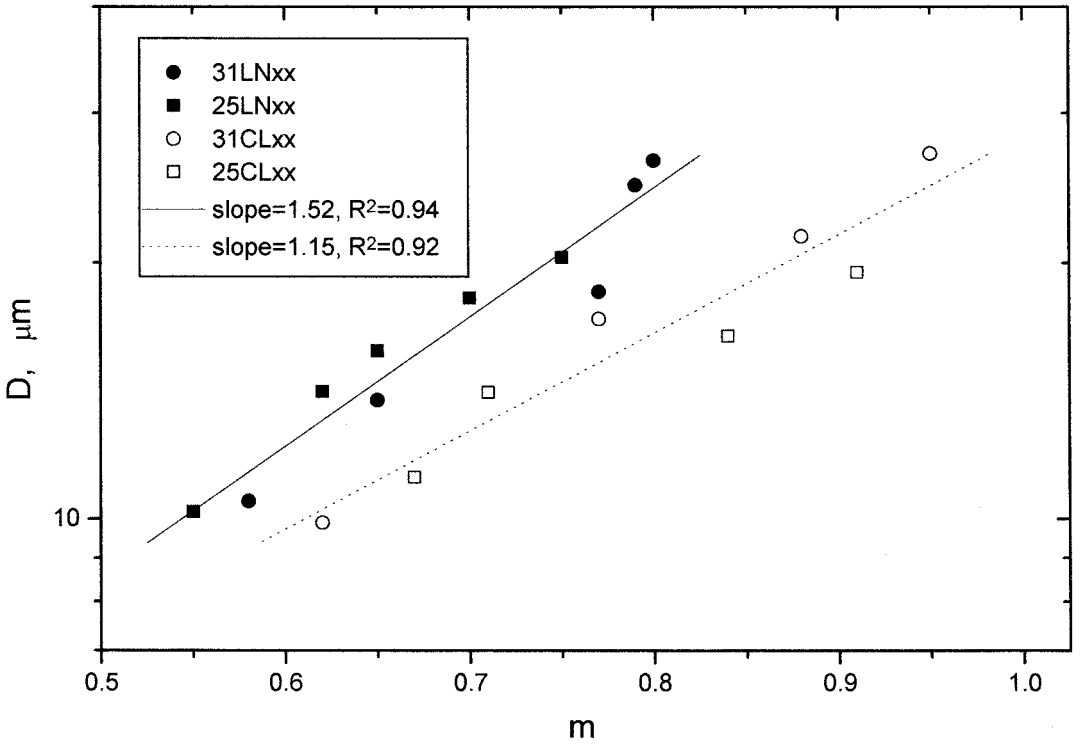

Figure 10 The variations of D versus m of all samples.

in which Ca is a capillary number, τ is a shear stress, σ is an interfacial tension, and R is the radius of the droplet. For rupturing of a droplet to occur, the capillary number must exceed a critical value (i.e., τ is higher than a critical value). By combining eqs. 2 and 5, we can gain

$$\log(D) = \log(2\mathrm{Ca}\sigma/\tau_{\mathrm{eff}}) = \log(2\mathrm{Ca}\sigma/A) - m\log(\dot{\gamma}_{\mathrm{eff}}) \quad (6)$$

in which $\mathrm{Ca} = \tau_{\mathrm{eff}}/(\sigma/R)$, $D = 2R$, $\dot{\gamma}_{\mathrm{eff}}$ is a strain rate under τ_{eff}, and $\tau_{\mathrm{eff}}(\tau_{\mathrm{eff}} = \tau - \tau_0 = A\dot{\gamma}_{\mathrm{eff}}^m)$ is a minimum stress that is needed to overcome the Laplace pressure and further to deform a droplet at flowing state. Equation 6 suggests that the plot of $\log(D)$ versus m is a line if $2\mathrm{Ca}\sigma/A$ and $\dot{\gamma}_{\mathrm{eff}}$ are constants. The plots of the data of yyCL-xx and yyEM-xx are shown in Figure 10, which and indicates a linear relationship between m and $\log(D)$. In Figure 10, the slope is equal to $-\log(\dot{\gamma}_{\mathrm{eff}})$, and $\dot{\gamma}_{\mathrm{eff}}$ are 0.03 and 0.07 s^{-1} for the emulsions and the colloidal solutions, respectively. The τ_{eff} can be obtained with the $\dot{\gamma}_{\mathrm{eff}}$ and eq. 2 ($\tau_{\mathrm{eff}} = \tau - \tau_0 = A\dot{\gamma}_{\mathrm{eff}}^m$, in which A and m are the constants shown in Figures 9a and 9b). These results reveal that for the emulsions (or the colloidal solutions), the strain rates $\dot{\gamma}_{\mathrm{eff}}$ that overcome the Laplace pressures are nearly the same, although the higher τ_{eff} is needed for the higher φ.

If $2\mathrm{Ca}\sigma/A$ is a constant, Ca is proportional to A/σ (i.e., $\mathrm{Ca} = \tau_{\mathrm{eff}}/(\sigma/R) = CA/\sigma$, in which C is a constant). Then, a relationship between τ_{eff} and A/D can be given by

$$\tau_{\mathrm{eff}} = C'A/D \quad (7)$$

in which C' ($C' = 2C$) is also a constant. Equation 7 suggests that the plot of $\log(A/D)$ versus $\log(\tau_{\mathrm{eff}})$ is a line and its slope is equal to 1. The plots of the data of yyCL-xx and yyEM-xx are shown in Figure 11 and indicate a linear relationship between $\log(A/D)$ and $\log(\tau_{\mathrm{eff}})$ as well as substantiates the slopes of the linear relationships are nearly equal to 1. These results support the assumptions (i.e., $2\mathrm{Ca}\sigma/A$ and $\dot{\gamma}_{\mathrm{eff}}$ are constants in eq. 6 of plotting a line of $\log(D)$ versus m in Figure 10).

CONCLUSIONS

(1) The yield stresses (τ_0) of the emulsions and the colloidal solutions are proportional to

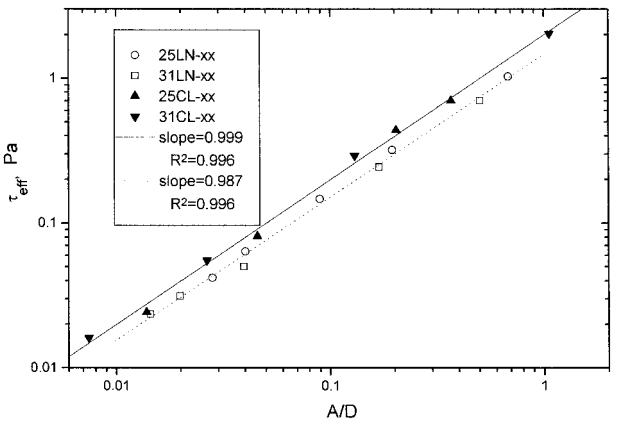

Figure 11 The relation between τ_{eff} and A/D.

$\varphi^{1/3}/D$ in the range $0.72 \leqq \varphi \leqq 0.81$. This result indicates the domination over the yield stresses to the attraction of droplets (or particles) in the stated range and extends the utilization of the theory of Princen and Kiss to the lower φ.

(2) The relations $\log(D) \sim m$ and $\tau_{eff} \sim A/D$ exist if $Ca\sigma/A$ and $\dot{Y}_{eff}$ are constants; this is confirmed by the data of the investigated samples with $0.62 \leqq \varphi \leqq 0.81$.

The authors thank Mr. Yong-Li Pan and Dr. Chen Chang for their help with the NMR imaging tests.

REFERENCES

1. Petersen, S. B.; Muller, R. N.; Rinck, P. A. An Introduction to Biomedical Nuclear Magnetic Resonance, Thieme Company, 1985.
2. Lauffer, R. B. Chem Rev 1987, 87, 901–927.
3. Brasch, R. C. Radiology 1992, 183, 1–11.
4. Lauffer, R. B.; Larsen, S. K. U. S. Patent 5,527,522, 1996.
5. Toft, K. G.; Friisk, G. A. J Pharm Biomed Anal 1997, 15, 973.
6. Wendland, M. F.; Saeed, M.; Lauerma, K.; Derugin, N.; Mintorovitch, J.; Cavagna, F. M.; Higgins, C. B. Magn Reson Med 1997, 37, 448.
7. Waigh, R. D.; Fell, J. T.; Anie, S. J.; Wood, B. U. S. Patent 5,380,514, 1995.
8. Hiemenz, P. C. Principles of Colloid and Surface Chemistry, 2nd ed.; Marcel Dekker: New York, 1986.
9. Mason, T. G.; Bibette, J. Phys Rev Lett 1996, 16, 3481.
10. Mason, T. G.; Bibette, J.; Weitz, D. A. Phys Rev Lett 1995, 10, 2051.
11. Mason, T. G.; Bibette, J.; Weitz, D. A. J Colloid Interface Sci 1996, 179, 439.
12. Princen, H. M.; Kiss, A. D. J Colloid Interface Sci 1989, 128(1), 176.
13. Princen, H. M.; Kiss, A. D. J Colloid Interface Sci 1986, 112(2), 427.
14. Hsu, J. P.; Liu, B. T. J Colloid Interface Sci 1998, 198, 186.
15. Pal, R. Chem Eng J 1998, 70, 173.
16. Pal, R. Chem Eng J 1997, 67, 37.
17. Chang, C. R.; Powell, L. J Fluid Mech 1993, 253, 1.
18. Rodriguez, B. E.; Kaler, E. W.; Langmuir. 1992, 8, 2376.
19. Morse, D. C.; Witten, T. A. Europhys Lett 1993, 22(7), 549.
20. Adams, J. W. Paintindia, Oct 31, 1996.
21. Clarson, S. T.; Semlyen, J. A. Siloxane Polymers; Prentice Hall: New York, 1995.
22. Vahidi, H.; Berry, D. R.; Harvey, L. M. Toxicol Lett 1998, 95, 159.
23. Lobner, D. J Neurosci Meth 2000, 96(2), 147.